

The H I Halo of NGC 891

R.A. Swaters, R. Sancisi, J.M. van der Hulst

Kapteyn Astronomical Institute, University of Groningen, P.O. Box 800, 9700 AV, The
Netherlands

Received _____; accepted _____

ABSTRACT

Neutral hydrogen observations of the nearby, edge-on spiral galaxy NGC 891 reveal the presence of an H I halo extending up to at least 5 kpc from the plane. This halo gas appears to rotate 25 to 100 km/s more slowly than the gas in the plane. If this velocity difference is due to the gradient in the gravitational potential, then it may serve to discriminate between disk and spheroidal mass models. The classic picture of a large outer flare in the H I layer of NGC 891 may no longer be valid.

A correlation is seen between the distributions of H I, H α and radio continuum emission, which supports, in accordance with galactic fountain models, the picture of a substantial disk-halo circulation related to the star formation activity in the disk of NGC 891.

There is now also clear evidence for the presence of a rapidly rotating ($v_{rot} \simeq 230$ km/s) disk or ring of H I in the central part of NGC 891.

Subject headings: galaxies: individual (NGC 891) — galaxies: ISM — galaxies: kinematics and dynamics

1. Introduction

NGC 891 is a nearby Sbc galaxy, seen almost perfectly edge-on. In recent years it has been studied in detail at various wavelengths and has become the key system for the study of the vertical distribution of the interstellar medium in a disk galaxy.

Early studies with the Westerbork Synthesis Radio Telescope (WSRT) showed the presence of a radio continuum halo (Allen, Baldwin, & Sancisi 1978) and of H I emission at large distances from the plane (Sancisi & Allen 1979, hereafter SA), later confirmed by VLA observations (Rupen 1991). This emission was interpreted by SA as due to a huge flare of the outer H I disk of NGC 891.

In the central region of NGC 891 the observations showed a deep H I depression, which was attributed, at least partly, to the effect of H I absorption. A CO nuclear ring or disk was discovered by Sofue, Nakai, & Handa (1987) and has more recently been confirmed and studied in detail by García-Burillo et al. (1992, hereafter GGCD) and García-Burillo & Guélin (1995), but no such central system was detected in H I by SA or Rupen (1991).

NGC 891 was re-observed with the WSRT for 12 times 12 hours between March 1988 and January 1989. This provided us with the most sensitive H I data for an edge-on galaxy to date. Here we present the two main findings of these observations: the H I halo and the central H I ring or disk of NGC 891. A more detailed description of the observations and of the results will be presented elsewhere.

2. The H I Halo

The map of the total H I column density superposed on the optical image (Fig. 1) shows a thin, high-density H I layer coinciding with the dust lane in the galaxy plane and wings extending up to about 2 arcmin on both sides (1 arcmin \simeq 2.8 kpc). The total

amount of H I above 30 arcsec is about $6 \cdot 10^8 M_{\odot}$, or $\sim 15\%$ of the total H I mass of NGC 891. This H I at large z -distances from the plane, already detected (but with much lower signal/noise ratio) by SA, had been interpreted as being part of a flaring H I layer at large radii. This conclusion was based on the kinematics of the H I, shown here in the position-velocity maps in the directions along (Fig. 2) and perpendicular (Fig. 3) to the major axis of NGC 891. The H I emission at large z -distances (Fig. 3) has, in fact, radial velocities close to the systemic velocity of NGC 891 and should therefore, according to the kinematical model adopted by SA, be located in the outer parts of the system and hence be part of a large flare. It is important to note that in this standard model cylindrical rotation is assumed, i.e. the gas at a given radius in the galaxy has a rotational velocity independent of its z -distance from the plane.

With the new, higher sensitivity H I observations and a more sophisticated analysis that makes use of a three dimensional modeling, we now have obtained a different, clearer picture of the vertical structure of the H I in NGC 891. Models have been constructed for a range of different inclination angles, outer flares and line-of-sight warps. The input values for the rotation curve and the radial H I density distribution have been derived directly from the data. The standard value of 10 km/s has been adopted for the velocity dispersion. The other parameters, disc scaleheight, inclination and position angles, have been used to produce best fit models for an H I layer with flare, warp and various inclinations. The models have been inspected and analyzed in the same way as the data cubes in order to make a full comparison with the 3-D observational data set. Some of the results are shown in Fig. 4 where each column shows representative channel maps for a given model. The flare, warp and slow rotation models shown here are for $i = 90^{\circ}$. The rightmost column shows the data for the north (approaching) side of NGC 891. The galaxy center is marked by the cross on the right. The top row shows the channel maps at the systemic velocity, the bottom row shows channel maps at the extreme velocity, close to the rotation velocity

of the system. These latter channel maps, in standard circular rotation models, show the H I at the line of nodes of the orbits in the sky plane where the line of sight is tangent to the orbits.

From Fig. 4, it is clear that the models obtained for a thin (FWHM= 20'') H I layer viewed at different inclination angles fail to reproduce the observations. An inclination angle as low as 80° would be needed to reproduce the thick distributions in the observed channel maps, but such a low inclination would be totally inconsistent with the well-established lower limit of $\simeq 88.6^\circ$ (cf. Rupen et al. 1987). Furthermore, at such a low inclination the V-shaped signature which is already noticeable at 87° is very prominent, whereas it is not seen in the data. The flare model does not reproduce the overall shape of the observed channel maps, in particular not the remarkably thin structure of the hydrogen in the extreme velocity channel. This thin structure is reproduced in the line-of-sight warp models, but these show a different shape and a bifurcation that is not seen in the data at the velocities closer to systemic. Undoubtedly, a warp is present in the outer parts, as one can see from the data in Figs. 1 and 4: the gas at $\pm 6'$ from the center is displaced to the west on the NE side of the galaxy by about $10''$, and on the SW side it is displaced to the east by about the same amount. It has the characteristic integral-sign shape also seen in other edge-on galaxies, but it looks much less pronounced. The test made with the present model is for a warp more oriented in the line of sight, which, if present, would explain the large symmetric z -extension. The models appear to rule out this possibility. We have also modeled combinations of warp, inclination and flare and none of these models was able to reproduce the data satisfactorily.

All the models described above are based on the standard assumption that the gas at large z heights rotates with the same velocity as the gas in the plane. The column next to the observed channel maps in Fig. 4 shows a model in which this assumption has been

dropped and the gas layer is made up of two components, a thin disk (i.e. a Gaussian z -distribution with a FWHM = 20'') rotating according to the derived rotation curve in the plane (Fig. 5), and a thick disk (Gaussian with FWHM = 80'') for which the flat part of the rotation curve is 25 km/s lower (see lower curve in Fig. 5). This model gives a better reproduction of the observations: both the general shape of the H I distribution and especially the thin structure in the channel map at the highest circular velocity (bottom row Fig. 4) are reproduced. A slight improvement is obtained if a larger value (20 to 30 km/s) is used for the velocity dispersion instead of the 10 km/s adopted here. In contrast to the flare model, this two-component model has gas in the halo region (thick component) everywhere above the thin disk. But, because of its lower rotation velocity, the thick component (or halo emission) does not show up in the extreme velocity channels as these correspond to the higher rotation velocity of the thin disk.

Such a model, with a thick component rotating more slowly than the thin disk, is likely to be overly simplified. It is more likely that there is a gradual decrease of the density and of the rotation velocity with increasing z height. In order to obtain an overall picture of such variations we have derived a ‘tangent-velocity field’ of the whole galaxy, in and above the plane, with the assumption that there is H I everywhere, filling the orbits at the nodes (where the line of sight velocity is maximal) for orbits of all radii. This model is a very simple configuration of stratified gas layers with no outer flaring. And, as usual for edge-on galaxies (cf. SA), at each position the rotation velocity is given by the velocity with the largest deviation from systemic, after correction for instrumental broadening and random motions. Fig. 5 shows the rotation curve for the gas in the plane (top curve) and the rotation curve above the plane (bottom curve). To derive the latter we have integrated over the strip $30'' < z < 60''$ and also averaged on the two sides of the galaxy to increase the signal/noise ratio. In the inner region these rotation curves, mainly because of the poor S/N ratio, are not well defined. The position-velocity diagram for the galactic plane,

shown in Fig. 2, indicates a very steep velocity rise near the center and a peak within 1 kpc radius, probably due to a central rotating disk or ring (see below). Farther out, between 2 and 5 kpc, there is a dip and a new rise to the flat part ($v_{rot} = 225$ km/s) of the curve. The rotation curve (Fig. 5) for the gas above the plane, derived under the assumption that there is gas at the line of nodes, is indeed, in its flat part, about 25 km/s lower. In the inner regions, between 4 and 10 kpc, the difference is much larger, up to 100 km/s. The rotation velocity (flat part) seems to decrease smoothly with increasing z -distance from the plane (cf. Fig. 3). A rough estimate of the vertical gradient is 20 km/s per kpc.

3. Discussion

The principal, new findings of these observations of NGC 891 are the H I halo and its slower rotation as compared to the H I in the plane. New questions now arise. What is the origin of this halo gas? What causes its slower rotation? Is there still, to some extent, a flare in the outer H I layer?

There is little doubt that the origin of this halo gas and its kinetic energy are related to the star formation activity in the disk of NGC 891 which is particularly intense, as indicated by the strong H-alpha (Rand, Kulkarni, & Hester 1990) and the radio continuum emission (Allen et al. 1978; Dahlem, Dettmar, & Hummel 1994). These components are, like the H I, quite extended in the z -direction. More recently, also diffuse hot X-ray gas has been found (Bregman & Pildis 1994). Further support of the view that a high star formation rate in the disk lies at the origin of a disk-halo gas flow comes from H I observations of galaxies seen face-on. In NGC 6946, where the star formation activity is also high, widespread high velocity H I with vertical motions of up to 100 km/s has been detected by Kamphuis & Sancisi (1993). All these H I observations, separately giving the edge-on and the face-on views, support the picture of a substantial disk-halo gas circulation

in spiral galaxies (Sancisi, Kamphuis, & Swaters 1996) in accordance with galactic fountain models (Bregman 1980).

Perhaps the strongest evidence linking the substantial disk-halo H I flow with the star formation activity in the disk of NGC 891, comes from the pronounced north-south asymmetry already seen in the radio continuum and in the H α maps mentioned above and now also found in H I. The considerably higher activity in the northern part of the galaxy is clearly manifested by the brighter and thicker radio continuum and H α there. A similar north-south asymmetry is now also indicated by the two maps (Fig. 3) which show the vertical position-velocity structure of H I for the north and the south sides of NGC 891. In both maps, the emission seen close to the systemic velocity and stretching up above 1 arcmin from the plane is from the slow-rotating halo identified above. At velocities closer to the maximum circular velocity, the H I layer looks clearly thicker in the north than in the south. A straightforward interpretation is that this is due to H I at intermediate z -heights (30-60 arcsec) which rotates almost as fast as the gas in the plane and is present only on the northern side of NGC 891 where the star formation activity is higher. It could be fresh gas flowing up from the plane and still connected with the fast rotating, low- z H I.

In summary, the similarity between the morphologies of the extended H α , the radio continuum and the H I is the best evidence, together with the kinematical information discussed above, that the H I is part of the halo and not of an outer flare.

It is not clear what may cause the slower rotation of the halo gas. The gravitational field, the structure and energy balance of the interstellar gas and the magnetic field are all likely to play a role. If the velocity structure of the gas at high z -distances from the plane is coupled to the gravitational potential, as in the plane, the observed decrease in azimuthal velocity with z and the non-corotation of disk and halo gas is revealing the vertical distribution of matter. It can be used, perhaps, to discriminate between disk and

spheroidal mass models. In this picture the largest decrease in azimuthal velocity would be expected at small radii, as indeed Fig. 5 seems to indicate. The disk-halo gas circulation may be understood in the light of galactic fountain dynamics (Bregman 1980; see also review by Spitzer 1990). The gas moves upward from the disk into the halo and radially outward conserving angular momentum and losing azimuthal speed. Alternatively, a large asymmetric drift would also cause a decrease of the rotational velocity of the halo gas. Here, however, it seems unlikely to have an important effect as the required large velocity dispersion (>50 km/s) is not seen in the H I data, but more sensitive observations would be needed to rule it out completely.

As to the flare, it should be understood that the present results do not rule out the possibility that the H I layer of NGC 891 may become thicker in its outer parts. The consequence of this work is that now the picture has become less simple and that the analysis required to extract the vertical density profile of the H I layer will be dependent on the kinematical model adopted.

4. The nuclear disk or ring

In the central region of NGC 891 there appears to be a depression in the H I density distribution (Fig. 1), which in itself would not be unusual in a spiral galaxy of such early type. But in this case the effect is enhanced by the absorption against the radio continuum and by the H I self-absorption. This effect is strongest near the minor axis because of velocity crowding. Also, note the absorption feature visible in the position-velocity map (Fig. 2 top) between 500 and 600 km/s at the position of the supernova SN 1986J (Rupen et al. 1987), about 1 arcmin to the SW of the center.

Near the center of NGC 891 the position-velocity map (Fig. 2) shows the presence of

faint emission at very low (NE side) and very high (SW side) radial velocities. This H I, not seen in the earlier, less sensitive observations, follows the pattern of the overall rotation of the galaxy with approximately the same amplitude. It has the unmistakable signature of a fast rotating disk or ring of gas with a radius of approximately $15''$ (700 pc) and coplanar with the galaxy disk. In the z -direction it is unresolved by the $12''$ beam: its thickness must then be much less than 500 pc. There is little doubt that this is the same rotating nuclear disk discovered in CO. Its estimated H I mass is $1 \cdot 10^7 M_{\odot}$, with a factor of two uncertainty. The radial velocity changes from 300 to 760 km/s. The maximum rotation velocity is 230 km/s, about equal to that of the main disk.

The value of the $M(\text{H}_2)$ to $M(\text{H I})$ ratio for the nuclear disk, obtained using the H_2 mass estimated by GGCD, is ~ 20 , similar to the value of ~ 30 for the Galactic nuclear disk (Combes 1991), but much larger than that of ~ 1 found for the whole disk of NGC 891.

We thank R. Bottema, F.H. Briggs, K.H. Kuijken and T.S. van Albada for valuable comments. The WSRT is operated by the Netherlands Foundation for Research in Astronomy with the financial support from the Netherlands Organisation for Scientific Research (NWO).

REFERENCES

- Allen, R. J., Baldwin, J. E., Sancisi, R. 1978, *A&A* **62**, 397
- Bregman, J. N. 1980, *ApJ* **236**, 577
- Bregman, J. N., Pildis, R. A. 1994, *ApJ* **420**, 570
- Combes, F. 1991, *ARA&A* **29**, 195
- Dahlem, M., Dettmar, R.-J., Hummel, E. 1994, *A&A* **290**, 384
- Dettmar, R.-J. 1990, *A&A* **232**, L15
- García-Burillo, S., Guélin, M. 1995, *A&A* **299**, 657
- García-Burillo, S., Guélin, M., Cernicharo, J., Dahlem, M. 1992, *A&A* **266**, 21
- Kamphuis, J. J., Sancisi, R. 1993, *A&A* **273**, L31
- Rand, R. J., Kulkarni, S. R., Hester, J. J. 1990, *ApJ* **352**, L1
- Rupen, M. P. 1991, *AJ* **102**, 48
- Rupen, M. P., van Gorkum, J. H., Knapp, G. R., Gunn, J. E., Schneider, D. P. 1987, *AJ* **94**, 61
- Sancisi, R., Allen, R. J. 1979, *A&A* **74**, 73
- Sancisi, R., Kamphuis, J. J., Swaters, R. A. 1996, in *The Interplay between Massive Star Formation, the ISM and Galaxy Evolution*, eds. D. Kunth, B. Guideroni, M. Heydari-Malayeri, Trinh Xuan Thuan, (Gif-sur-Yvette: Editions Frontières), p. 205
- Sofue, Y., Nakai, N., Handa, T. 1987, *PASJ* **39**, 47
- Spitzer, L. 1990, *ARA&A* **28**, 71

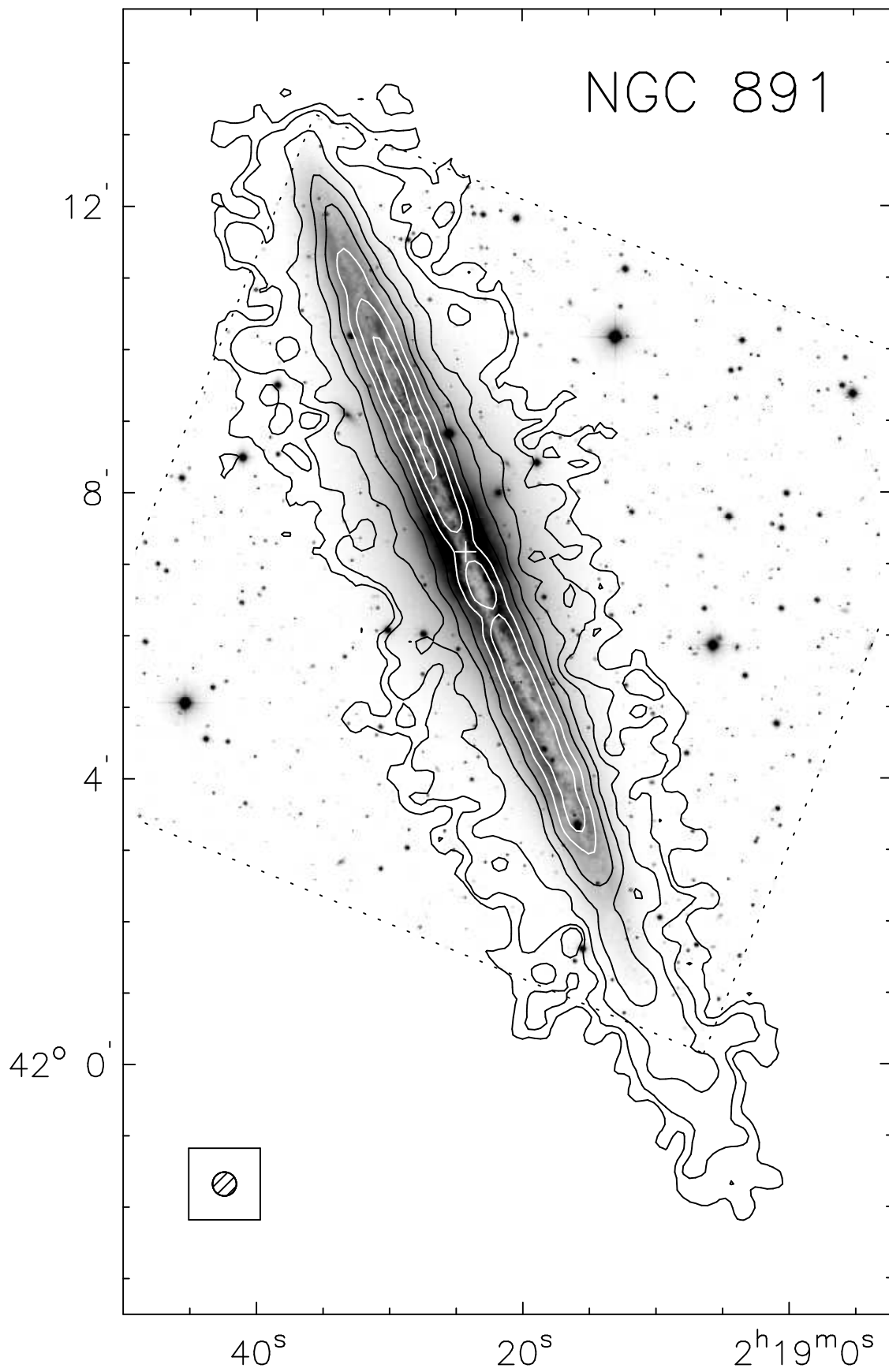
Fig. 1.— H I map of NGC 891 superposed on the optical image (courtesy of Balcells & Swaters). The contours are 0.07 ($\simeq 1.5\sigma$), 0.17, 0.46, 1.1, 2.3, 4.1, 6.4, $9.2 \cdot 10^{21}$ H I atoms cm^{-2} . The cross indicates the position of the central radio continuum source. The HP beamwidth is $20''$. The dotted line indicated the edge of the CCD frame.

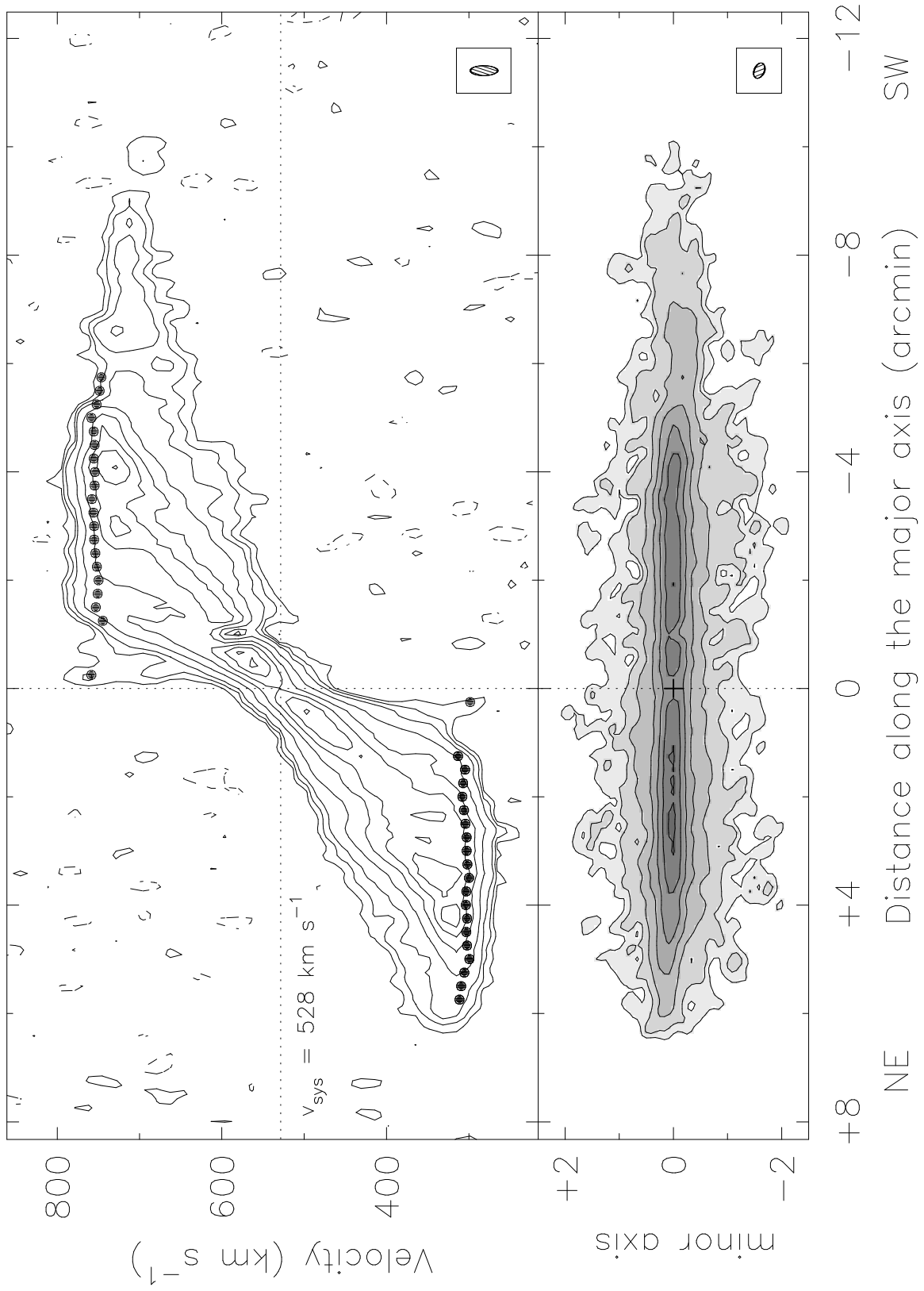
Fig. 2.— Top: Position-velocity map along the major axis of NGC 891. The dots show the rotation curve (see Fig. 5). The contours are -0.6, 0.6 (2σ), 1.2, 2, 5, 10, 15, 20, 25 mJy/beam. The angular and velocity resolutions are $15''$ and 33 km/s (FWHM). Bottom: H I map of NGC 891 at full resolution ($17.8'' \times 11.2''$). Contours are 0.14 ($\simeq 1.5\sigma$), 0.35, 0.9, 2.3, 4.5, 8.3, $12.9 \cdot 10^{21}$ H I atoms cm^{-2} .

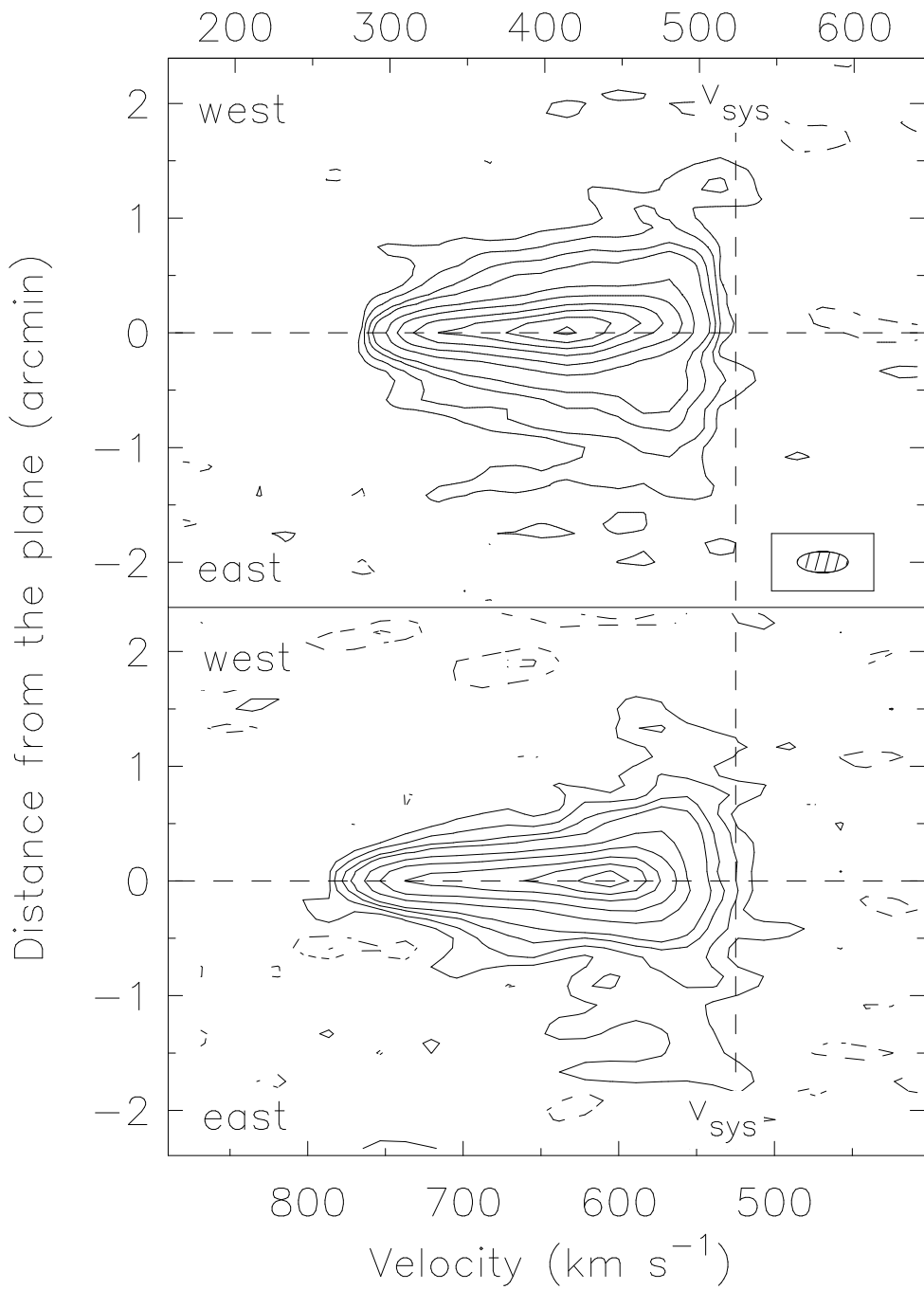
Fig. 3.— Position-velocity maps perpendicular to the major axis for the north (top) and south (bottom) sides of NGC 891. They have been obtained by integrating over strips parallel to the major axis from $1.25'$ to $2'$ from the center. The angular and velocity resolutions are $12''$ and 33 km/s (FWHM). Contour levels are -5.6, -2.8, 2.8 (2σ), 5.6, 8.4, 15, 30, 50, 80, 110, 140, 170 mJy/beam. Velocities are heliocentric. The vertical dashed line indicates the systemic velocity of NGC 891 (528 km/s).

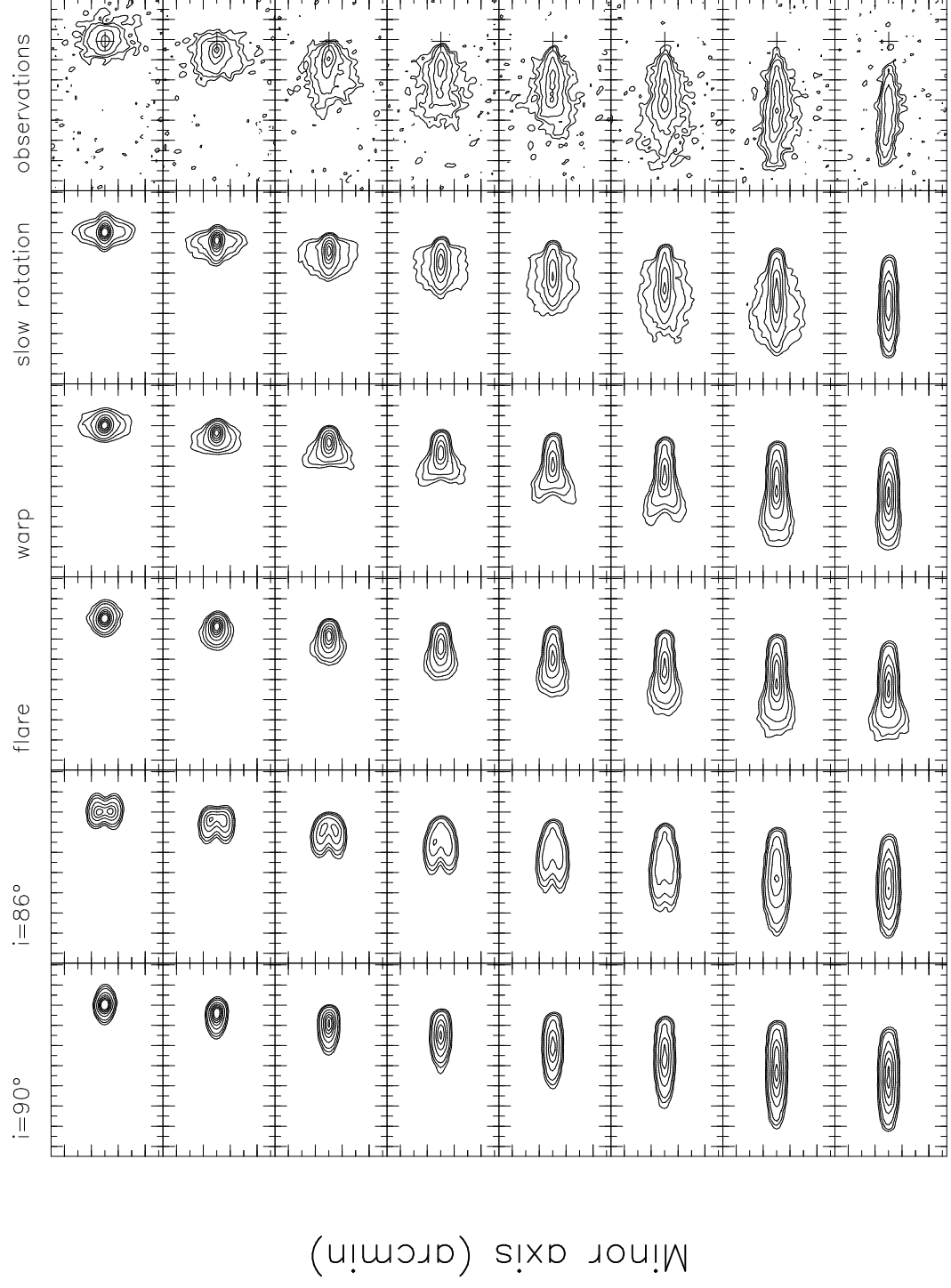
Fig. 4.— Representative channel maps from different models and from the observations of the northern (approaching) side of NGC 891. The channel radial velocities run in steps of 33 km/s from systemic (528 km/s, heliocentric) at the top to near rotational (299 km/s, hel.) at the bottom. The contour levels are -0.62, 0.62 (2σ), 1.24, 2.5, 5, 10, 15, 20, 25 mJy/beam. The HP beamwidth is $11.2'' \times 17.8''$. The centre of NGC 891 is marked by the cross on the right.

Fig. 5.— The rotation curve of NGC 891 for the gas in the plane of the galaxy (filled circles) and for a strip from 30 to 60 arcsec above and below the plane (open circles). Both curves are north-south averages.









Minor axis (arcmin)

Major axis (arcmin)

